Engineering and Applied Sciences
2024, Vol. 9, No. 1, pp. 14-33
https://doi.org/10.11648/j.eas.20240901.12

Research Article

Sustainability and Resiliency Investigation of Grouted Coupler Embedded in RC ABC Bridge Pier at Vehicle Impact

Suman Roy*

Department of Civil and Environmental Engineering, Utah State University, Logan, Utah, U.S.A

Abstract

Increased occurrences of natural and man-made dynamic loading caused by high strain rate dynamic impact load have been recently reported. Different statistical results indicate that vehicular impacts occur more frequently compared to the other dynamic loads. However, existing literature primarily focuses on enhancing survivability and determining damage levels specifically in relation to faster bridge construction methods used as an accelerated bridge construction (ABC). In this context, the present study investigates the dynamic behavior of a commonly used connection type in ABC, namely grouted coupler that connects pre-cast elements like bridge piers and foundations. To execute the research, both the static and dynamic performance of grouted couplers embedded in pier foundation subjected to high strain rate loading incurred by high velocity vehicular impact are examined. A representative non-traditional reinforced concrete (RC) bridge pier is selected for the study with the standardized geometry and selected material properties. The use of splice sleeves as coupler materials and specified cross-sectional hollow cast iron cylinders filled with high strength concrete grout is employed for developing Finite Element (FE) modeling, extracting data from published journals. A commercial software, ANSYS, has been utilized to develop FE models to capture post impact respective static and dynamic behaviors, and the simulation results are then compared with the analytical. This also includes determining material performance via FE simulations. By considering dynamic loading, the dynamic impact factor (DIF) has been evaluated for the reinforcing steel bar adjacent and embedded into the coupler. In addition, dynamic simulations, and material modulus in demand to sustain impact are determined. Thus, the research necessitates mesh-independent sensitivity studies to investigate DIF corresponding to the precise outcomes. The findings of this study manifests valuable information that aids to opt for the suitable coupler connections, considering material properties, and adequate post impact execution. Consequently, it will serve as a useful design tool for design offices, structural practitioners, and forensic structural engineers.

Keywords

Non-Traditional ABC Bridge Pier, High Velocity Vehicle Impact, Grouted Coupler, FEM, and Validation of FE Model

1. Introduction

Bridge piers experience highly dynamic impact due to seismic events, blast, and vehicular collisions. This may cause health deterioration of the bridge pier from less to severe, and possibly collapse. Structural evaluation for seismic performance has received significant attention in high earthquake prone states in the region comprising primarily of the western United States of America (USA) [20]. The seismic behavior and response of traditional reinforced concrete (RC) bridge

*Corresponding author: sumanroy74@gmail.com (Suman Roy)

Received: 30 December 2023; **Accepted:** 12 January 2024; **Published:** 7 March 2024

pier has been the subject of extensive research efforts executed to improve the capacity of the piers to high strain rate deformation due to seismic loading [1]. Unfortunately, the other mechanisms of dynamic impacts, like, vehicular collisions, and blast load have received little attention. This leads an additional insight to look into the RC bridge pier performing on dynamic load exerted by small duration impact [15]. Different studies show that vehicular collisions with bridge elements are the most common dynamic impact scenario, especially with the increasing volumes of vehicular traffic [34]. The performance of the coupler has been investigated for both dynamic and static combined stresses for various vehicle impact scenarios. Quasi-static to dynamic strain rates of reinforcing steel bar connected to the couplers is also evaluated and published in [30]. To characterize damage incurred by vehicle crash is subjected to the concrete strength parameters quantifying a good tradeoff between the shear capacity to primarily resist the impact load [28], and the flexural capacity controlling principal serviceability of the pier [29]. However, this present study intends to quantify the coupler post impact behavior at high strain rate load incurred by semi-trailer on the representative prototyped and half-sized ABC pier utilizing grouted coupler.

In addition to the seismic load, the other dynamic loading scenarios, such as blast and car crash also warrant investigation and thorough inspection. Precisely, vehicular impact calls for significant attention due to a high frequency of occurrence [33]. Recently, this has been observed that crashworthiness by vehicle impact jeopardizes direly the health, and hence reduces serviceability of the pier. With regards to vehicle impact loading encountered by RC bridge piers, the majority of the existing literature focuses on identifying severity of damage levels [27, 34]. While this research is valuable, the performance of RC bridge piers under vehicle impact has yet to be fully investigated for recent developments in terms of materials and construction methods such as ABC. In this method, connectors such as splice sleeves and grouted couplers are commonly used to connect different bridge components such as foundations to piers. The introduction of these new materials, splice sleeves and grouted couplers, differ the dynamic response of bridge structures due to the fact that they typically behave higher stiffness's than steel rebar, result in discontinuities of the reinforcing steel within the coupler and change the energy dissipation path [23, 29]. In addition, grouted coupler and splice sleeve connectors facilitate the construction of RC bridge but their use in plastic hinge location is restricted as specified in seismic bridge design codes [5]. This study has been performed to address the material properties and its contribution to the post impact performance at impact. In addition to introduce new materials and construction methods, the performance levels of the bridge-piers assessment under multi-hazard effects has yet to be thoroughly researched. Sequential or simultaneous hazardous loading experienced by circular RC bridge pier due to blast and vehicular impact have already been investigated in terms of the performance and resistance reduction method [39].

However, precise assessment of splice-sleeve and grouted coupler used in ABC needs an additional attention in using coupler proposed by Utah Department of Transportation (UDOT) before its widespread use [6]. To analyze the impact characteristics of grouted coupler, it is placed in the pier-foundation connection in order to evaluate the performance standard of the splice sleeve and grouted coupler mechanism as a composite material [23]. The performance of splice sleeve was further reported in the proposed literature by 'Idaho Transportation Department' [12]. A study of the structural reliability of RC piers subjected to sequential loading exerted by blast and vehicular impact were also studied. The study showed that the structural performance of the piers are particularly sensitive to its dimensions [31, 39]. This implies that an increase in the stiffness of the pier could possibly help it withstand the external forces caused by vehicular impact. Coupler sections have been studied as a means of increasing the stiffness of the RC piers to improve their seismic performance and overcome the development of plastic hinges [38, 39]. However, the effect of these couplers on the response of RC bridge piers subjected to vehicle impact loading is a complex mechanism and still relatively unknown. This study is an attempt to evaluate the performance of individual grouted coupler section against short duration impact to predict the coupler behavior, and material properties as well. In the present study, splice-sleeves along with high grade concrete grouted coupler are embedded into the pier-foundation, placing the foundation top and the coupler cross-section in the same level, as shown in Figure 1. However, plastic hinges are expected to form in the weakest part of the pier, predicting dissipation of maximum energy [23], particularly at the pier-foundation junction as predicted and specified [12]. Performance of single pier due to dynamic impact exerted by vehicle collision on it, undergo high frontal overpressure [15]. As such, failure mechanism of each coupler along with the material properties need rigorous prior investigation before recommending its widespread use in foundation-pier connection for ABC under axially compressive stress, and the combined stresses resulting from residual flexure caused by impact load, transferring it at pier base [40, 41].

The importance of this present study is to examine static and dynamic characteristics of the single coupler material used in RC bridge pier at vehicle impact. To assess post impact behavior and enhance the post impact performance level, study of coupler on dynamic load needs further insight. The study further helps to determine post impact performance reliability by utilizing dynamic impact factor (DIF), carried out from finite element models (FEM) from manufacturer supplied material properties, and results from experimental testing. The FEM simulations are used in this study to determine the DIF of the single coupler under axial compression and horizontal shear load typically experienced from vehicle impact. This present study is an accomplishment to investigate the performance ABC pier at vehicle impact to determine

necessary bridge calibration.

2. Methodology

In this research, splice-sleeve and grouted coupler embedded in a foundation cap connecting the reinforcing steel bar has been evaluated at vehicular impact loading. Quasi-static to dynamic strain loading has been incorporated to investigate. The grouted coupler's impact performance has been evaluated for the dynamic load incurred by semi-trailer. Prototyped ABC pier with lower concrete strength has been utilized [27] to estimate damage of the coupler-steel bar region incurred by impact. The impact of the pier specimen is subjected to the concrete strength parameters due to its high vulnerability to vehicle impact due to its exposed surface area quantifying a good composition between the shear capacity to primarily resist the impact load, and the flexural capacity predominately control the serviceability of the pier [29, 32]. However, this present study intends to quantify the coupler at high velocity post vehicle impact behavior at impact load.

Performance level comprising of material properties and post impact behavior are determined by fractioning the load transmission per coupler. The investigation is carried out through numerical simulations via FEM utilizing the material properties from manufacturer's data. To examine the material behavior and failure pattern against vehicle impact, short duration post impact performances are evaluated through static and dynamic numerical simulations of the single coupler and validated with the manufacturer provided experimental results to compute the dynamic impact factor (DIF). Commercially available software package, ANSYS WORKBENCH, has been used to carry out the respective static and dynamic simulations. The respective DIFs computed using numerical simulations and from analytical methods are compared to validate the results from published journals.

2.1. Material and Geometric Properties of Splice-sleeve

Various connection types have been studied for precast concrete bridge piers in seismic areas and designated in two major categories of emulative and rocking connections [21]. The emulative connection for precast components is specified as a connection that includes special detailing. This type of splice-sleeve predicts better performance to withstand dynamic impact for reproducing a monolithic cast-in-place component.

For this particular study, geometrical details of splice sleeve recommended and typically used in ABC connector is 8U-X and is as shown in Figure 1 and Table 1. Splice-sleeve used for grouted coupler in the column rebar embedded and placed (Figure 2) within the pier foundation, predicts enhanced performance in dynamic response [19].

For this study, sleeve number 8U-X is considered and investigated as recommended for # 8 ASTM 706 bars used in pier for main reinforcement [27].

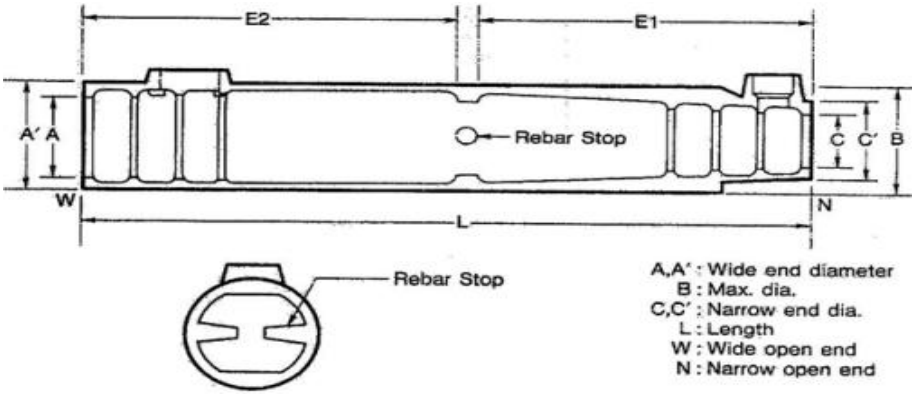

Figure 1. *Splice-sleeve [22].*

Table 1. *Details of splice sleeve number 8U-X [22].*

Zone	Coupler Type	Internal Diameter (in.) (mm)	External Diameter (in.) (mm)
W = Wider End	8U-X	1.89 (48.01)	2.52 (64.01)
N = Narrower End	8U-X	1.3 (33.02)	2.52 (64.01)

2.2. Placement of the Grouted Coupler

The grouted couplers are strategically placed in the location where plastic hinges are likely expected to form, i.e., at the pier-foundation connection [12]. The pier section with grouted coupler is shown in Figure 1 (b). Splice-sleeves (Figure 1) considered from manufacturers catalogue, and grouted couplers are placed and embedded into the foundation are as shown in Figure 2 (a & b). Both ends of the pier are modeled with fixed supports and the location of vehicle impact is considered at a distance 3 feet height from the foundation top.

3. Dynamic Impact Performance of ABC Bridge Pier

Cast-in-place bridge pier like RC or ABC experiences highly dynamic impact due to seismic response, blast, and vehicular collision [1, 3].. This may cause health deterioration of the pier from less and moderate to severe, till collapse. From different studies and captured data from published journals [14], frequency of vehicular collision causing crashworthiness seems surpassing the other dynamic responses [41]. High velocity vehicular impact and its post effect on the traditional RC bridge pier has received attention. On the other hand, performance of ABC using splice sleeve along with high grade concrete grouted couplers at high velocity vehicle impact are relatively unknown. Performance of the pier and the dynamic impact on it are studied for axially compressive stress and the combined stresses as a result of residual flexure due to impact at pier base. The coupler region must exhibit adequate stress limit over the dynamic stresses for service. Grouted couplers in plastic hinge zones must develop 150% [38] of the specified yield strength of the connected reinforcing bar. Stresses are computed from finite element (FE) modeling to assess the coupler performances using high strain rate deformation [13]. High strain-rate deformation is considered especially as far as the impact and shocking load is concerned where the rate sensitivity leads to the high stresses causing enhanced stresses, resulting dislocation. At the specific higher strain rate loading, the mobile dislocation velocity increases to accommodate the required plasticity [1].

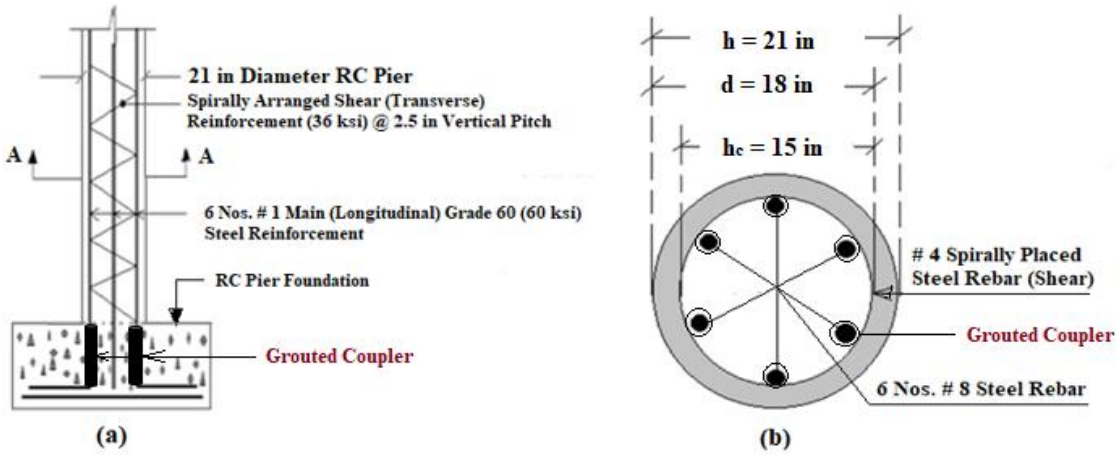

Figure 2. *(a) Grouted coupler and splice sleeve position position in ABC RC pier, and (b) Section A-A.*

3.1. Determination of Flexural Properties

The representative RC pier is designed by utilizing a concrete grade of 3 ksi and longitudinal reinforcement (primary) of grade 60 steel (60 ksi tensile strength) considered from the published data [30], and for the shear reinforcement (transverse), grade 36 steel (36 ksi tensile strength) is used [16]. Sectional elevation of the RC pier and details of the pier cross-section are shown in Figure 2(a & b). End conditions are considered and utilized in pier are both ends are restrained against displacement and rotation in all directions, and unrestrained length of the pier is taken as 8.5 feet with circular cross-section throughout ("Grouted Splice Sleeve Connectors for ABC Bridge Joints in High-Seismic Regions – Transportation Blog" n.d.), as shown in Figure 3(b). The pier has primary reinforcement of 6 numbers # 8 steel re-bars throughout the foundation bottom, followed by a spirally arranged shear reinforcement with # 4 steel (grade of 36 ksi) rebar @ 2-1/2 inches pitch throughout as utilized in the representative pier ("Grouted Splice Sleeve Connectors for ABC Bridge Joints in High-Seismic Regions – Transportation Blog" n.d.). Shear reinforcement provided in the pier conforms to the minimum shear reinforcement criteria [2]. In addition, the representative pier also satisfies the minimum shear reinforcement criteria for steel bar diameter and pitch of the spiral reinforcement [18].

In this study, flexural performances of the coupler embed-

ded at concrete foundation base is estimated. Tables 1 and 2 include computations of axial loads on pier and respective each reinforcing steel bar. Splice-sleeve details are already shown in Table 2, and DIF of steel bar is shown in Table 3. Computations of axial compressive load experienced by RC pier and individual coupler are shown respectively in Tables 2 and 3. Semi-trailer has been considered as a vehicle weight [4] for impact from the data given and as included in Table 4. Computation of the axially compressive load incurred by the RC circular bridge pier, as shown in Figure 2(b) [i.e., Sec A-A of Figure 1 (a)], is given in Equation 1 [17].

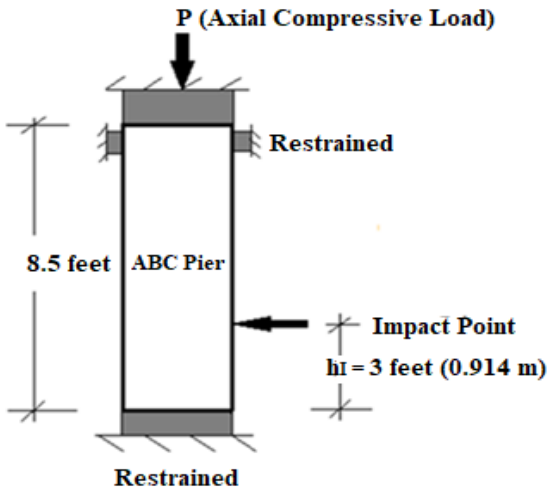

Figure 3. *Impact Point and boundary conditions of the representative ABC bridge pier.*

Direct axial and static compression load ($P_{n,d}$) of the pier can be computed from Equation 1.

$$P_{n,d} = 0.85f_c'(A_g - A_{st}) + A_{st}f_y \quad (1)$$

Where: A_g and A_{st}, indicate gross cross-sectional area of pier and the area of reinforcing steel rebar in pier section, and f'_c and f_y are the respective strengths of 28 days concrete in compression and reinforcing steel rebar in tension.

The resulting values of axial compressive load experienced by the RC pier is as shown in Table 2.

Table 2. *Materials and Geometric Properties.*

f'_c (ksi) (MPa)	f_y (ksi) (MPa)	A_g (in^2) (mm^2)	A_{st} (in^2) (cm^2)	$P_{n,d}$ (kips) (kN)
3 (20.68)	60 (413.68)	346.50 (2235.48)	4.70 (30.32)	1310 (5827.17)

The resulting value of axial compressive load experienced by the RC pier has been fractioned, and the apportioned axial load incurred by the individual coupler conforming individual material and geometric properties can be computed from Equation 2.

$$P_{n,s} = P_{n,d}\left[\frac{A_{CI}.E_{CI}+A_{Grout}.E_{Grout}}{A_{net}.E_{Concrete}+A_{st}.E_{st}}\right].\eta \quad (2)$$

Where: $P_{n,d}$ and $P_{n,s}$ are the respective design axial compression capacities of RC pier and individual steel rebar; A_{CI}, A_{st}, and A_{Grout} indicate gross cross-sectional area of cast iron component of the coupler, area of reinforcing steel rebar in pier section, and cross-sectional area of grout. and cross-sectional area of hollow splice-sleeve; E_{CI}, E_{Grout}, $E_{Concrete}$, and E_{st} express material modulus of cast iron of splice-sleeve, grout, concrete, and reinforcing steel rebar; and η is the energy dissipation after impact. To analyze the coupler behavior, $E_{Concrete}$ is considered as 2.65 psi, and the respective values of E_{CI}, E_{Grout}, and E_{st} as considered in this study are as shown in Table 5.

The equation 2 yields an apportioned axial compressive load of 3.1 kips incurred by each coupler and has been used to investigate its performance at impact load.

$A_{coupler}$ signifies the summation of the cross sections of hollow splice sleeve (cast iron) and grout. From geometry and using Figures 4 and 5, $A_{coupler}$ can be deduced from the relation as shown in Equation 3.

$$A_{coupler} = A_{CI} + A_{Grout} \quad (3)$$

Where: $A_{coupler}$ is the cross-sectional area of grouted coupler; A_{CI} and A_{Grout} indicate area of hollow splice sleeve (cast iron) and cross-section of the grout.

Using Table 1, and Figures 4 and 5, $A_{coupler}$ can be evaluated as 2.20 in^2 (14.20 cm^2).

Although the material moduli of cast iron and reinforcing steel are much higher than that of concrete and grout, but their respective cross-sectional areas are very less as compared to pier that triggers the negligible effect of material moduli controlling the impact effect. In addition, immediate effect during impact, shear primarily controls the post impact behavior and is followed by axial load after impact which is a complex mechanism. Direct axial compression load from pier via individual reinforcing steel rebar ($P_{n,s}$) to coupler is transmitted and approximately evaluated by fractioning down the column axial load, using the area ratio ($A_{coupler}/A_{net}$), as shown in Equation 3. However, axial load being a secondary controlling factor of impact behavior, a negligible amount of fractioned axial compression load (η is approximately considered as 0.2% due to dissipation effect) has been received by the coupler composite system. In order to mitigate the effect of material modulus in impact, the simplification of Equation 2 resulting approximately the same result withing 2.9% variation is as shown in Equation 4.

$$P_{n,s} = P_{n,d}\left(\frac{A_{coupler}}{A_{net}}\right) \quad (4)$$

Where: $P_{n,d}$ and $P_{n,s}$ are the respective design axial compression capacities of RC pier and individual steel rebar; A_{net}, and $A_{coupler}$ indicate net cross-sectional area of pier, and cross-sectional area of couple composite.

The resulting apportioned values of axial compressive load experienced by the RC pier and partitioned load incurred by individual coupler conforming material and geometric properties (given in Table 2) using Equations 1, 2, 3 and 4 are shown in Table 3.

Table 3. *Design values of respective axial loads.*

P_n (kips) (kN)	$P_{n,d}$ (kips) (kN)	$P_{n,s}$ (kips) (kN)
1308.20 (5819.16)	1310 (5827.17)	3.01 (13.38)

3.2. Determination of Dynamic Increase Factor (DIF)

The dynamic increase factor (DIF) used in this study is termed as the ratio of the dynamic to static strength of the element [9]. Reinforcing steel bar being an isotropic and homogeneous material can dissipate high energy and carries out substantial impact load [29]. In this research, a representative RC (ABC) pier specimen (Figure 2) has been considered for investigation at impact. Vehicle weight (M) and impacting velocity (V) of the semi-trailer are considered as 42,108 lbs (187.30 kN) and 100 ft/sec (30.48 m/sec) respectively and permissible vehicular velocity has been extracted and considered from the standardized permissible vehicular speed [19, 36]. Determination of dynamic increase factor (DIF) as a consequence of vehicular impact and corresponding dynamic performance of steel re-bars are studied at quasi-static strain rate condition. Dynamic flow stress (σ_{dyn}) in steel at impact has been determined by the following Equation 5, as recommended [15]:

$$\sigma_{dyn} = \sigma_y \left[1 + \left(\frac{\dot{\varepsilon}}{C}\right)^{1/p}\right] \quad (5)$$

Where: σ_y is a static flow stress of for ASTM A 706 [7] using Grade 60 reinforcing steel bar and is considered as 60 ksi (420 MPa); C is the material coefficient and p is the strain rate parameters with the values are considered as 40 and 5 respectively [35]. Quasi-static to high strain rate of steel bar ($\dot{\varepsilon}$) has been approximately considered as 0.16 s^{-1} for the vehicle velocity 100 ft/sec (30.48 mtr/sec) [36] to assess the post impact scenario from the time of collision considering high strain rate non-linear loading, and ductile behavior as the RC pier is under the axial compression and experiencing of transverse load [37]. From Equation 3, Dynamic flow stress (σ_{dyn}) has been evaluated as 79.8 ksi (550.20 MPa).

Using Equation 3 and, the dynamic parameter 'ξ' can be computed by using the Equation 6 [25, 26].

$$\xi = 0.019 - 0.009 * \left(\frac{\sigma_{dyn}}{60}\right) \quad (6)$$

Where: ξ is a dynamic parameter which depends on the dynamic yield stress of steel at the strain hardening zone, and σ_{dyn} is the dynamic flow stress at uni-axial plastic strain rate of steel.

However, ξ is evaluated as 0.0172 after replacing σ_{dyn} (using Equation 4) as 79.8 ksi.

Dynamic Impact Factor (DIF) can be evaluated from Equation 7 by using ξ computed from Equation 5 [21, 26].

$$DIF = \left(\frac{\dot{\varepsilon}}{10^{-4}}\right)^{\xi} \quad (7)$$

Where: DIF is the Dynamic Impact Factor, ξ is dynamic parameter, and $\dot{\varepsilon}$ is the Quasi-static strain rate of steel re-bar.

Equation 5 yields the analytical DIF result as 1.053.

3.3. Computation of Analytical Static and Dynamic Forces of Coupler

Static impact force (I_S) due to vehicular collision can be computed from Equation 8.

$$I_S = \frac{WV}{t} \quad (8)$$

Where: I_S is the static impact force, W is the semi-trailer weight (42108 lbs or 19099.87 kg-wt); V is the maximum permissible impact velocity considered as 100 ft/sec (30.48 m/sec) [15] and t is impact duration considered as 40 ms (milli-second) [10] in this present study, and h_I is the height of impact from foundation top as shown in Figure 3.

Inserting values in Equation 6, yields I_S as 105270 kip-ft/sec^2 or 142114.50 kN-m/sec^2 (corresponding equivalent load is 3271.896 kips or 14554.12 kN) [8, 10].

Corresponding static moment (M_s) exerted by the pier from vehicle impact can be determined by using Equation 9.

$$M_s = I_S . h_I \quad (9)$$

Where: M_s represents the static moment incurred by RC ABC bridge pier, and h_I is the height of impact at pier considered from the foundation top.

By using load apportioning method after multiplying M_s (as shown in Equation 8) by the area ratio ($A_{coupler}/A_{net}$), the static moment experienced by single coupler ($M_{s,c}$) can be approximately determined from using Equation 10.

$$M_{s,c} = M_s\left(\frac{A_{coupler}}{A_{net}}\right) \quad (10)$$

The corresponding approximate dynamic moment experienced by single coupler ($M_{dyn,c}$) has been evaluated from Equation 11 in order for carrying out the analytical model.

$$M_{dyn,c} = DIF.M_{s,c} \quad (11)$$

Where: $M_{s,c}$ and $M_{dyn,c}$ represent static and dynamic moments experienced by single coupler from vehicle impact via load transmittance, and DIF represents the dynamic increase factor.

Equation 10 yields static single coupler moment ($M_{s,c}$) as 22.257 kip-ft (30.17 kN-mtr). The corresponding dynamic coupler moment ($M_{dyn,c}$) is computed from Equation 11, yields 23.437 kip-ft, (30.18 kN-mtr), and are as shown in Table 4. As the dynamic properties cannot be estimated directly due to short duration collision, it can be indirectly estimated by using DIF of reinforcing steel bar used in the RCC [24].

Table 4. *Computation of Coupler Moment (AFDC 2018).*

I_S (kips) (kN)	h' (feet) (m)	M_s (kip-ft) (kN-m)	DIF	M_{dyn} (kip-ft) (kN-m)
3271.89 (14554.12)	3 (0.91)	22.26 (30.16)	1.053	23.44 (31.78)

Computed fractioned loads for axial compression ($P_{n,s}$) as computed for individual steel bar is of 3.01 kips (13.40 kN) and has been already discussed in Section 3.1. The apportioned transverse load at the free end of individual steel rebar (8 in. edge, as shown in Figure 4) developed from the static moment (M_s) from vehicle impact, which in furtherance incurs moment at coupler-steel bar junction in pursuance of conservative analyses (Tables 2 and 4) yields as 22.257 kip-ft. (31.54 kN-m). This results substantial stress in the coupler-steel bar junction resulting high deformation (as shown in Figure 11).

However, in this study, static and corresponding dynamic analyses are performed, and each result is compared to predict the material properties in demand with the impact scenario. Dynamic properties cannot be measured directly due to short duration collision and non-linear trend, but using DIF, dynamic moment ($M_{dyn,c}$) at coupler-rebar junction can be well estimated. This also is subjected to significant stress (as shown in Figure 5) developed in coupler rebar junction as a post effect of short duration impact. However, energy dissipation occurs substantially during and immediate after the impact controls pier behavior and addressed the corresponding failure pattern [24]. The performance of the plastic failure zone as corresponding to its stiffness warrants flexural members as it governs the load capacities of the post impacted member [41].

4. Finite Element Modeling (FEM) for Grouted Coupler

In this study, finite element modeling (FEM) has been extensively used to predict the individual coupler performance at vehicle impact. The commercial FE software 'ANSYS' is used for performing static and explicit dynamic analyses to develop FE models for simulations and to obtain respective results. In order to develop the model, hollow cylindrical cast iron splice-sleeve (36 ksi or 248 MPa) is used along with 6 ksi (41.36 MPa) grouting and # 8 reinforcing streel rebar embedded into the grout, as shown in Figure 2. For all different material's connections, composite section is considered for developing the model. The mesh size considered for the simulations followed after mesh-independence is considered as 0.01 in. (0.254 mm). Steel rebar's conforming specified yield strength (60 ksi or 420 MPa) are embedded and extended from coupler in both sides are 8 in. (20.32 cm) and 6 in. (15.24 cm) respectively, as shown in Figure 4. The external surface of the splice-sleeve model is considered as fixed in the peripheral surface as it is embedded and placed in the foundation concrete. The free end of the 6 in. side is also considered as fixed (as shown in Figure 4) as it is extended within the foundation and received adequate development length.

To compare the DIF's computed from numerical simulations comprising of FEA model with the analytical results, stress ratio (σ_{dyn} / σ_{static}) is considered using steel strain rate from Equation 4. The peripheral surface of the grouted coupler is considered as no lateral displacement in any directions as it is embedded in concrete, and hence considered to be fixed the equivalent fractioned forces are applied to the larger end of steel bar of the model as shown in Figure 4. Apportioned horizontal impact (shear) and axial forces (flexure) are deployed on the model from the respective external moment and axial compressive force of pier at the free end (8 in. edge of steel bar from pier base or foundation top within pier) and is shown in the respective Tables 3 and 4. Load conditions along with the boundary conditions of coupler-steel bar model are also shown in Figure 4.

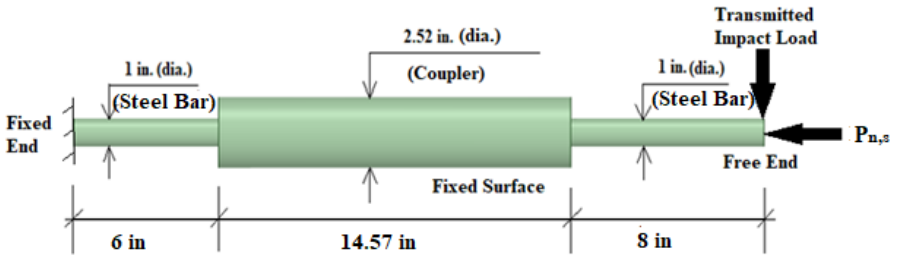

Figure 4. *End conditions and Load model for FEM of coupler-rebar.*

Material properties incorporating composite model for addressing splice sleeve and grouted coupler used in this study are developed and carried out using numerical modeling (FEM) under vehicle impact. The various material properties utilized in this study are extracted from manufacturer's data and are as shown in Table 5.

Table 5. *Material properties utilized for FE Modeling.*

SL. No.	Properties	Cast Iron	Grout	Steel Rebar
1	Density (pci) (kN/m^3)	0.284 (77)	0.083 (22.53)	0.284 (77)
2	Young's Modulus (psi) (MPa)	29*10^6 (2*10^5)	43.51 (0.3)	29*10^6 (2*10^5)
3	Poisson's Ratio	0.3	0.3	0.3
4	Bulk Modulus (psi) (MPa)	2.42*10^7 (1.6*10^5)	2.26*10^6 (1.6*10^4)	2.42*10^7 (1.6*10^5)
5	Shear Modulus (psi) (MPa)	1.12*10^7 (7.7*10^4)	1.84*10^6 (1.26*10^4)	1.12*10^7 (7.7*10^4)
6	Tensile Yield Strength (psi) (MPa)	3.62*10^4 (249.6)	0	3.62*10^4 (249.6)
7	Tensile Ultimate Strength (psi) (MPa)	3.62*10^4 (249.6)	0	6.67*10^4 (459.8)
8	Compressive Ultimate Strength (psi) (MPa)	0	5.95*10^3 (41.02)	0

4.1. Meshing of Grouted Coupler

Square mesh is considered for the entire grouted coupler and rebar model (as shown in Figure 5) along with splice-sleeve undertaken for the analyses as 0.01 in., for all elements. Mesh sizes are further reiterated from 0.1 in., and 0.05 in. respectively to carry out the sensitivity analyses showing if any variation exist. For all three different materials and their attachments, non-separable contact has been incorporated to act as a monolithic behavior of the model under vertical axial compression and horizontal impact for modelling flexure and shear. During simulation, high frictions are developed at the contacts of all inter material surfaces. The coupler-rebar model considered in this study shows large deformation because of transmitting horizontal load while RC bridge pier experiences high strain rate velocity vehicle impact load. Figure 5 shows FE model representing the grouted coupler and rebar consisting of mesh size of 0.01 in^2 (0.254 mm^2). Results are evaluated in terms of static and dynamic performances of the grouted coupler experiencing transmitted impact from RC bridge pier hit by high velocity semi-trailer.

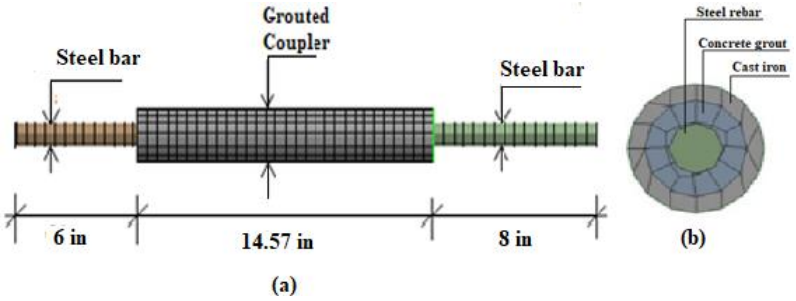

Figure 5. *Meshing of FEA Modeling for grouted coupler (a) longitudinal view, and (b) top view.*

4.2. Mesh Sensitivity Study of FEM

Mesh independence analyses are performed for respective mesh sizes of 0.1 in., 0.05 in. and 0.01 in, where results from strain and total deformation are considered for both static and dynamic considerations. Mesh independence with proximity is observed from the results comprised by numerical simulations developed by using ANSYS model for both static and dynamic considerations. In the present study, simulation is performed for individual mesh size, and is considered for the optimization. Results depicting from the mesh independence study to carry out sensitivity analyses involving different mesh sizes and compare with the results of the total deformation and equivalent strain are shown in the respective Figures 6, 7, and 8 incorporating deformations and corresponding equivalent strain. Mesh sensitivity studies to incorporate static results are precisely shown in Figure 6, whereas the results from dynamic performance comprising deformation and strain for different mesh sizes are shown in Figures 7 and 8 respectively. Different mesh sizes for pursuing sensitivity analyses show the results are within proximity. However, in this study, 0.01 in^2 (0.254 mm^2) mesh sizes are considered for static and explicit dynamics analyses using commercial software package, ANSYS. Figures 7 and 8 address results for time dependent total deformations and maximum strain concerning respective mesh sizes of 0.1 in^2, 0.05 in^2 and 0.01 in^2. Results illustrating static and dynamic analyses incur mesh independent and sensitivity study, determine total deformation and strain in the grouted coupler model embedded within the RC bridge pier experiencing vehicle impact.

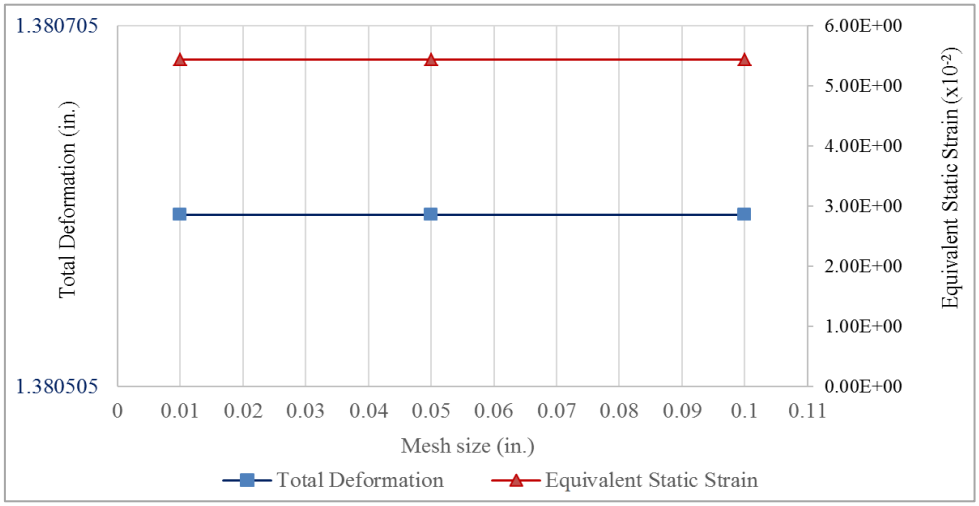

Figure 6. *Mesh Sensitivity for Total Deformation and Equivalent Strain (Static).*

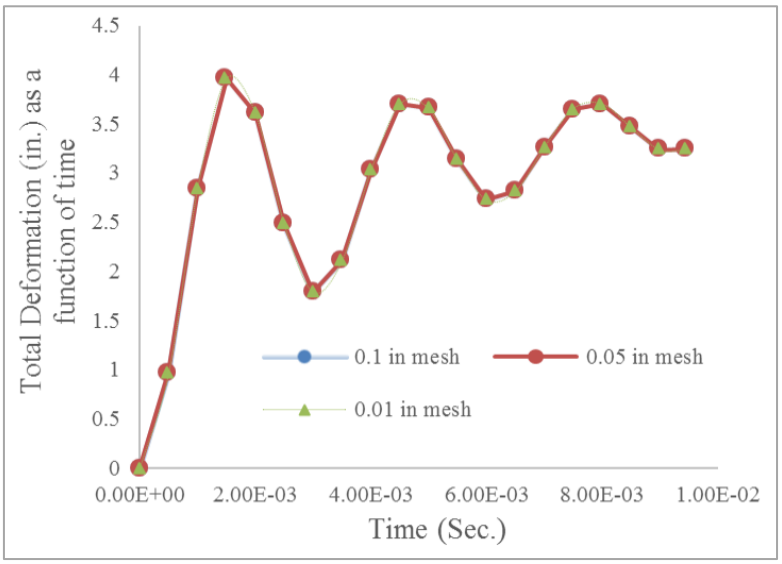

Figure 7. *Mesh Sensitivity for Total Deformation (Dynamic).*

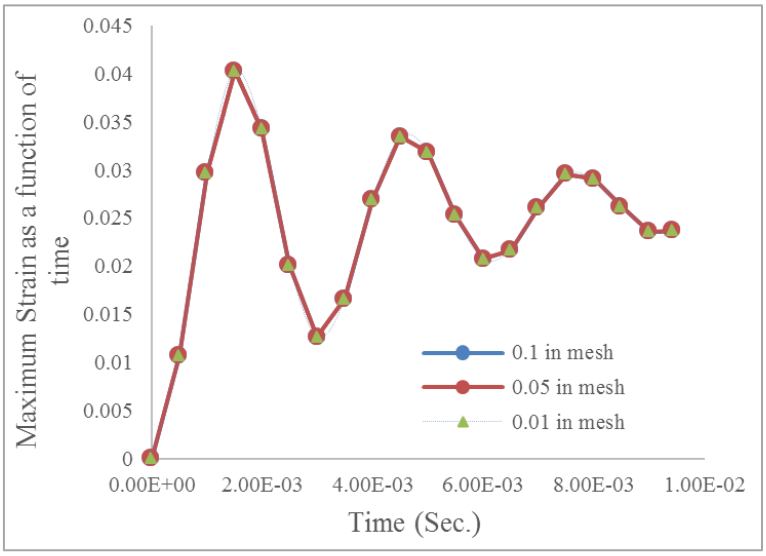

Figure 8. *Mesh Sensitivity for Maximum Strain (Dynamic).*

4.3. Uncertainty Assessment Using Confidence Interval (CI)

Confidence Interval (CI) has been utilized to capture the degree of uncertainty for assessing the numerical results evaluated from dynamic simulation using normal distribution. CI is also able to evaluate the probability that a parameter falls between a pair of values around the mean. Thus, the confidence interval (CI) is utilized to assess uncertainty, and determined via using mean (μ), standard deviation (SD), confidence level (z) and sample size (N) (as shown in Table 5) and is as shown in the Equation 12 [11].

$$CI = \mu \pm z.\frac{SD}{\sqrt{N}} \quad (12)$$

Where: μ is the mean of sample size, SD is the standard deviation, N is the sample size considered as one thousand data, and z is the confidence or significance level considered as 98%.

CI data to capture the uncertainty is shown in Table 6.

Table 6. *Input Data for CI.*

Input Variables	σ_D (psi)	εD	E_D (psi)
Significance Level (z)	0.02	0.02	0.02
Mean (μ)	668798.4	0.023975	32417194
Standard Deviation (SD)	628000	0.008989	628000
Sample size (N)	1000	1000	1000

5. Results

5.1. Results Using Finite Element Model (FEM)

Modeling's in furtherance of analyzing for stress induced, governing strain and deformation are carried out by using commercial software package, ANSYS, in order for performing static and explicit dynamic simulations. Static analyses are conducted for both scaled-down axial compression and the impact experiencing by each grouted-coupler and reinforcing steel rebar. Further analyses using explicit dynamics are also undertaken and the results including stress, strain and deflection are compared with the results from statics. Substantial deformations are observed from the results of both static and dynamic analyses. However, almost the failure is identified at the junction of steel rebar and coupler, and observed from the deformations in both the directions, parallel and perpendicular to the load of 1.375 in. (34.925 mm) and 0.119 in. (3.023 mm) for static (Figure 12), and 2.38 in. (60.45 mm) and 0.11 in. (2.794 mm) for dynamic (Figure 16), respectively.

5.1.1. Results Showing Finite Element Model in Performing Static Analysis

Results from static analysis present considerable deformation at the steel rebar. Deformations in both X and Y directions seem uniform, as 0.12 in. (0.004 mm.) and as shown in Figure 8. High strain concentrations and significant stress are observed in the contact of grouted coupler and steel rebar as shown in the Figures 9 and 11. Maximum permissible modulus of elasticity (material modulus to be considered as Maximum stress / Maximum strain) requirements from the simulation results subjected to static strain is 1.38 (Figure 10) and static stress (Figure 11) is $8.51*10^5$ psi ($5.8*10^3$ MPa),

whereas modulus of elasticity for steel rebar at the coupler junction demands as $6.17*10^5$ psi ($7.57*10^5$ MPa), which endorses material property safe enough as material E-modulus incorporating rebar in this study has been considered as $29*10^6$ psi. Time-dependent static strain and stress are shown in Figure 12. However, maximum strain and stress concentration at coupler-rebar junctions are considered for conservative approach and safety.

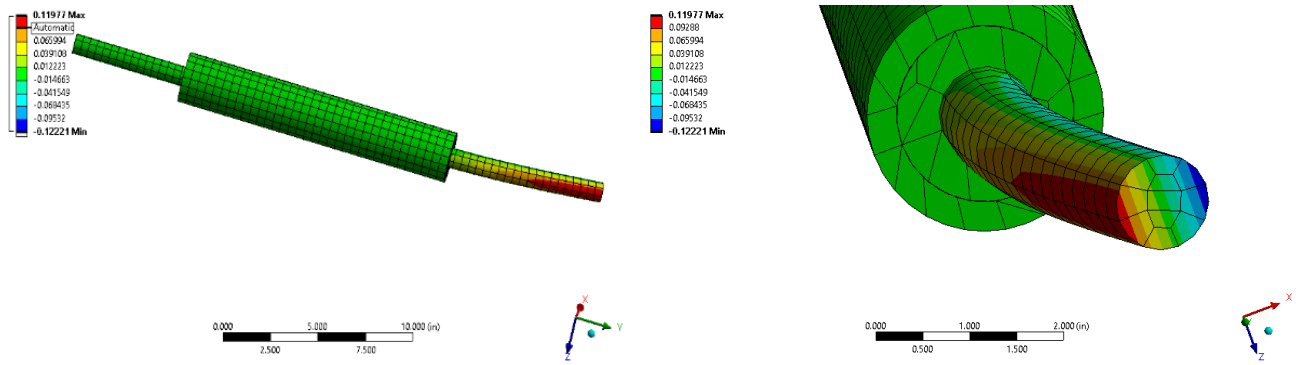

(a) (b)

Figure 9. *(a). Directional deformation in X-axis; (b). Directional deformation in Y-axis.*

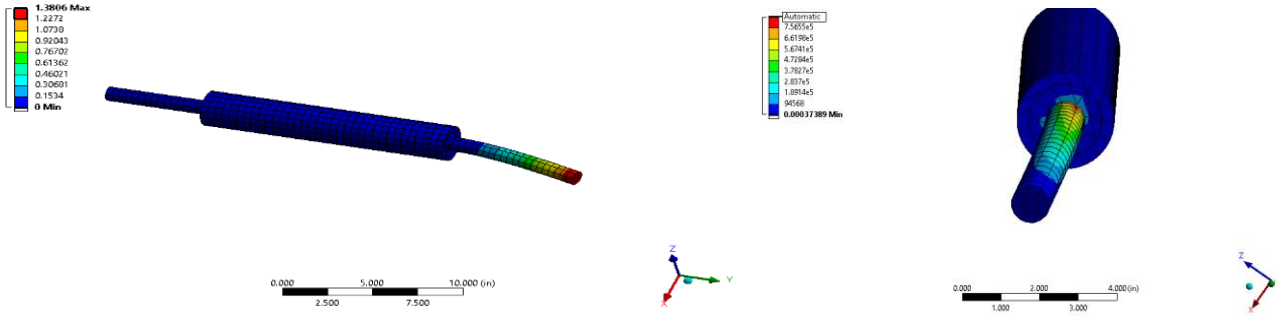

Figure 10. *Static strain.*

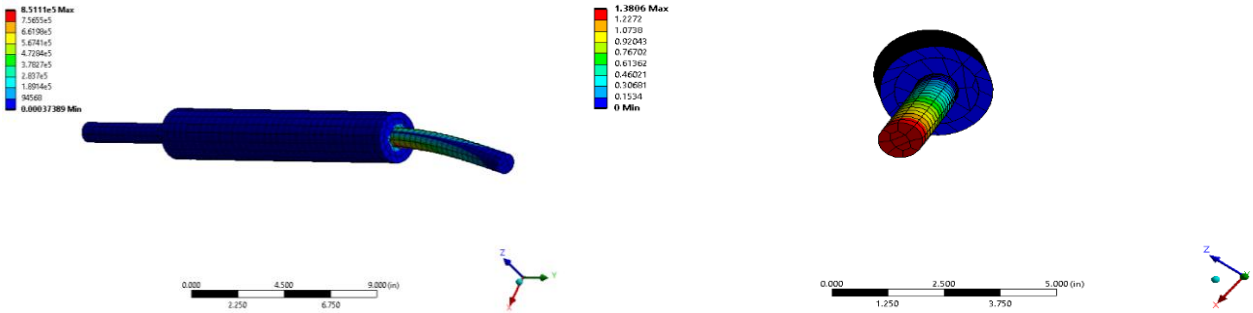

Figure 11. *Static stress.*

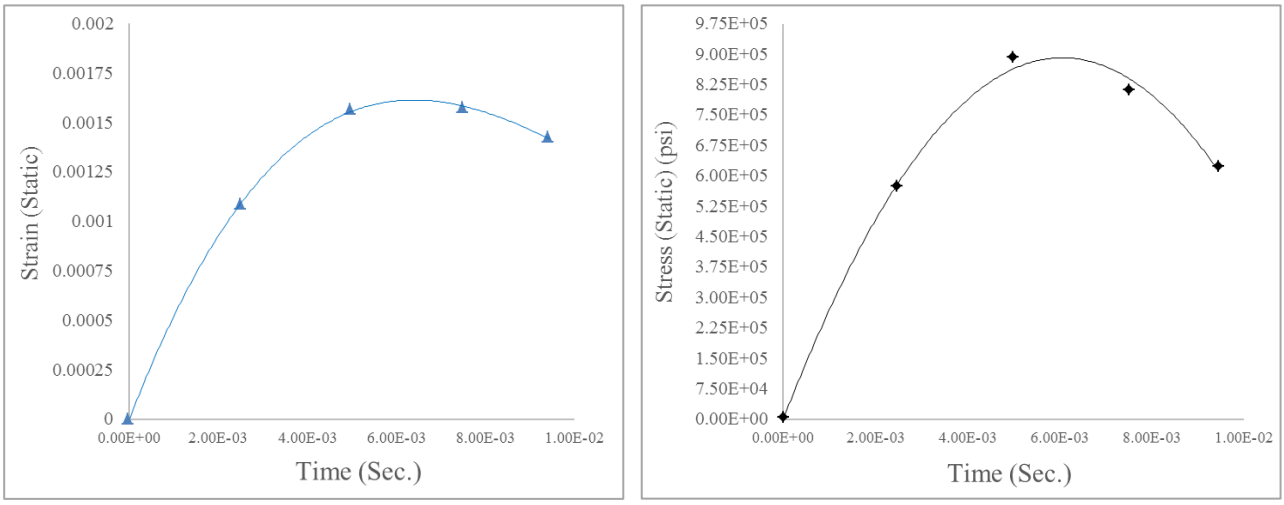

(a) (b)

Figure 12. *(a). Time-dependent Static Strain; (b). Time-dependent Static Stress.*

5.1.2. Results Showing Finite Element Model in Performing Dynamic Analysis

Results from dynamic analyses show significant deformation at steel rebar with high stress and strain concentrations at the contact of grout and steel rebar, as shown in Figures 13 to 15. In analyses, directional deformations seem quite different in the respective directions (3.15 in. and 0.12 in. along X and Y directions as shown in Figures 12 (a) and 12 (b)). Maximum permissible modulus of elasticity [Maximum Dynamic Modulus = Maximum dynamic stress / Max. dynamic strain)] requirements from simulation results subjected to dynamic stress and strain are $6.25*10^5$ psi ($1.82*10^5$ MPa), and 0.2 which exceeds material E-modulus incorporating rebar in this study. Using maximum dynamic stress (Figure 14) over dynamic strain, material modulus demand (maximum dynamic stress / maximum dynamic strain) is computed as $31.25*10^6$ psi ($2.15*10^5$ MPa), whereas material E-modulus considered as $29*10^6$ psi ($2.1*10^5$ MPa). However, demand of material modulus for dynamic over modulus captured from FE analysis is computed as 1.07, whereas the numerical DIF has been computed as 1.053 which commends a decent proximity between material and dynamic property. This result demands higher material modulus of reinforcing steel bar to execute improved performance on impact without undergoing large deformation. However, stress concentrations and strain shown at grout are remarkably high that controls design parameters. However, significant bond failure or spalling are not observed from the results albeit steel bar and grout experience higher strain followed by large deformation. Time-dependent static strain and stress are shown in Figure 16. However, conservative approach to determine maximum instantaneous strain and stress concentration at junctions are considered to avoid variations.

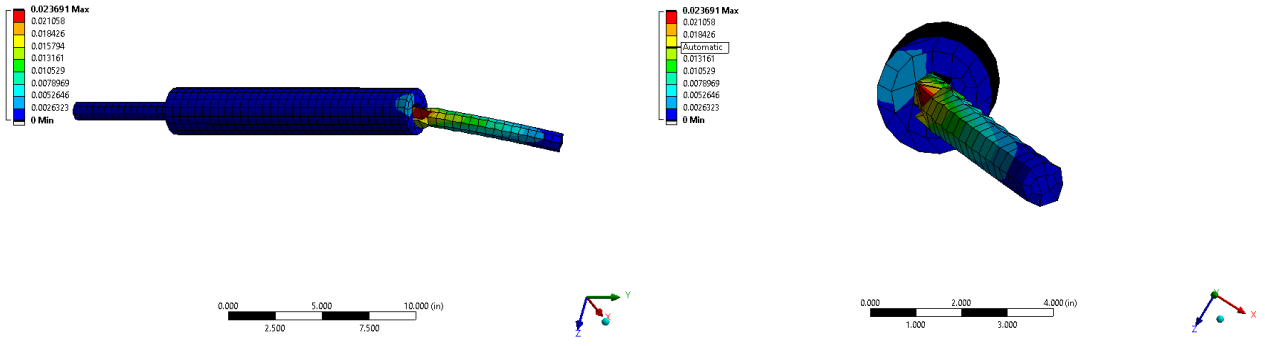

(a) (b)

Figure 13. *(a). Directional deformation in X-axis; (b). Directional deformation in Y-axis.*

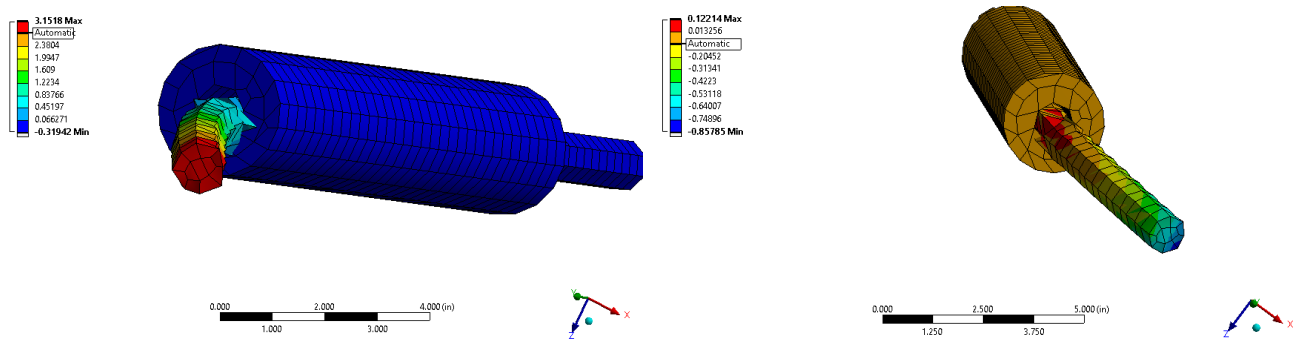

Figure 14. *Dynamic Strain.*

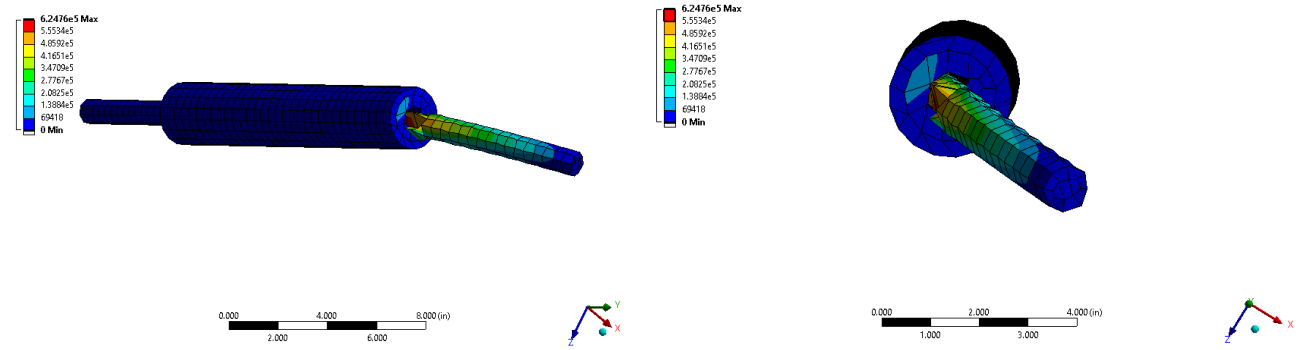

Figure 15. *Dynamic Stress.*

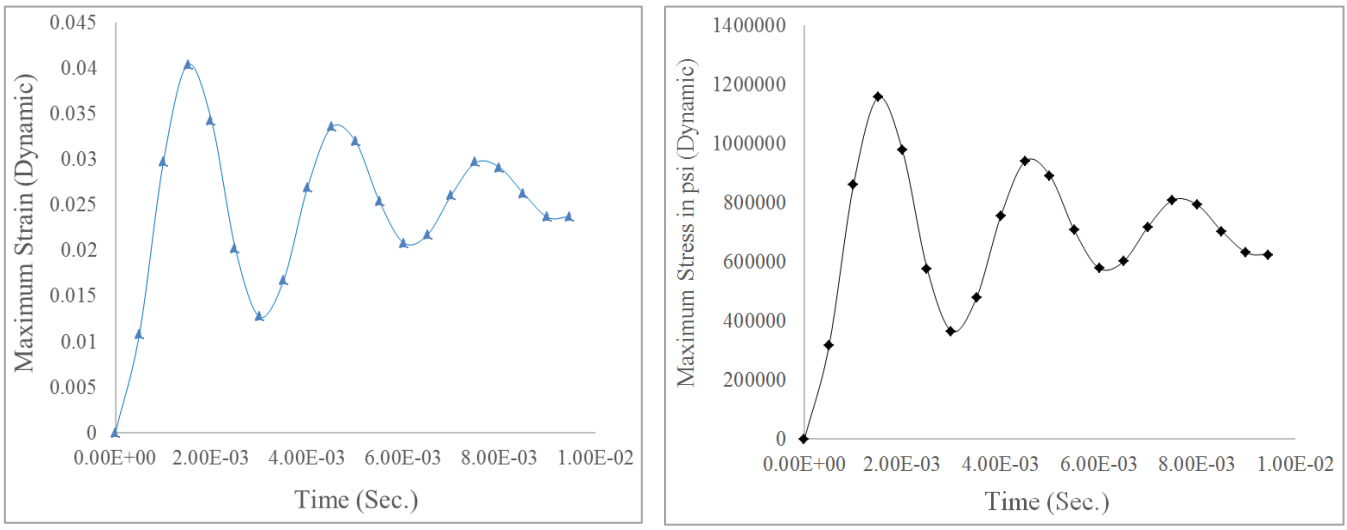

(a) (b)

Figure 16. *(a). Time-dependent Dynamic Strain; (b). Time-dependent Dynamic Stress.*

Time-dependent dynamic deformations are also captured from utilizing explicit dynamic simulations. Significant plastic deformations as the result of dynamic impact load application parallel and perpendicular to it are as shown in Figures 17(a) & 17(b). Deformation that takes place parallel to the load seems significantly higher than that of the perpendicular. However, in order for avoiding variations in deformations in different directions as a function of time, dynamic simulation to determine maximum plastic deformation is considered for being safety, and as a part of conservative approach. in different directions.

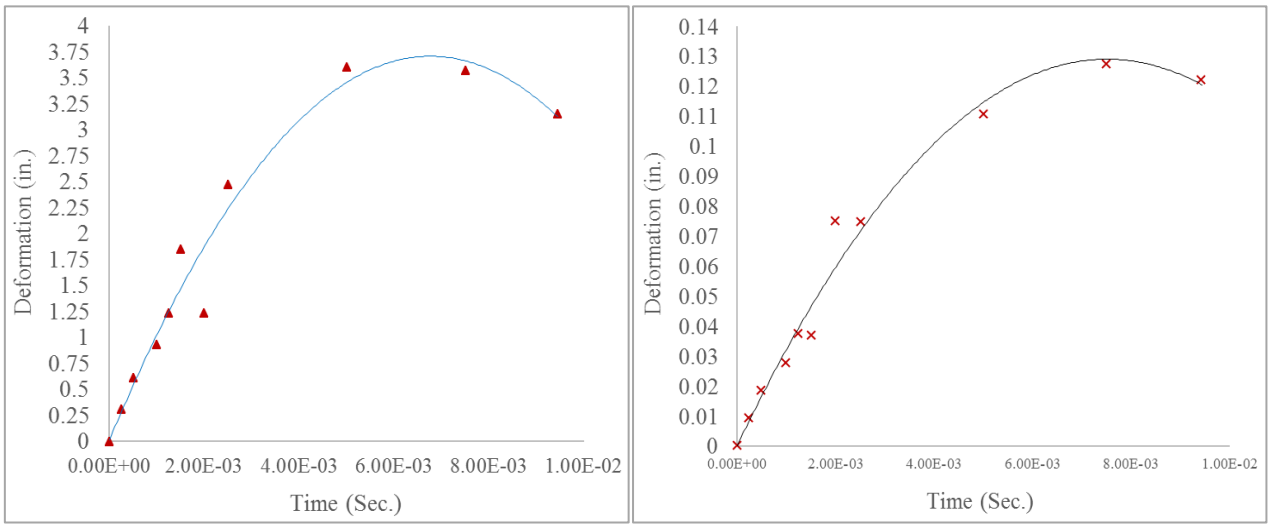

(a) (b)

Figure 17. *(a). Deformation parallel to load; (b). Deformation perpendicular to load.*

5.1.3. Results Showing Coupler Performing from Dynamic Analysis

Von Mises stress and corresponding strain plotted from dynamic simulations can capture the material property (dynamic modulus of elasticity) via regression analysis, come up with non-linear trend of performance function (g) of dynamic stress concentration and the corresponding dynamic strain are as shown in Figure 18.

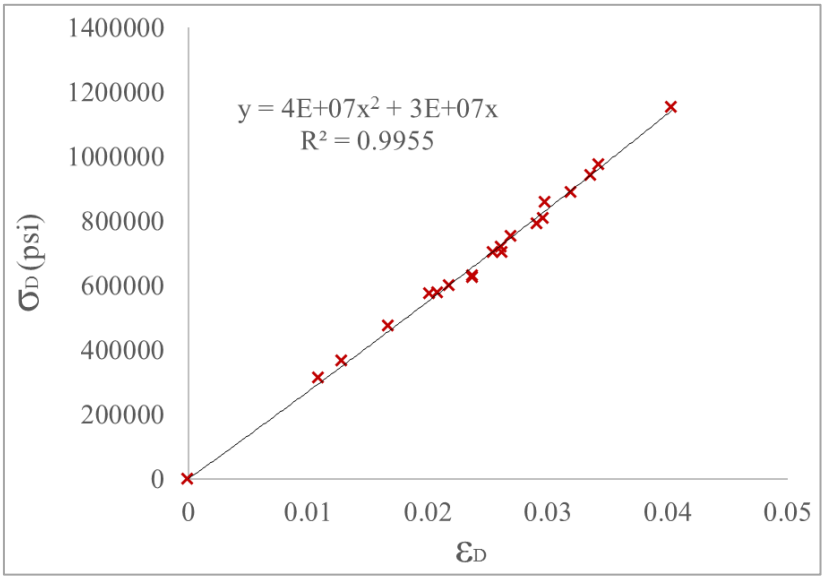

Figure 18. *Dynamic Stress and Strain Relationship to capture material properties.*

From Figure 18, regression results plotted with R^2 value of 0.99 to capture post impact performance of coupler is as shown in Equation 13.

$$g(\sigma_D, \varepsilon_D) = \sigma_D - 4.10^7.{\varepsilon_D}^2 - 3.10^7.\varepsilon \qquad (13)$$

Where: σ_D is the dynamic stress concentration at the pier due to impact and ε_D is the dynamic strain, and g is the post impact performance function.

5.2. Integrity Analysis of the Model

Due to variations in static and dynamic simulations results and complexities involved to capture material modulus as a post impact performance, and exceedance of dynamic over static and material modulus, dynamic results for material

modulus as demand are considered to capture post impact criteria. The mean (μ), covariance (V) and standard deviation (SD) of dynamic simulation results used to determine post impact performance integrity from dynamic stress and strain are shown in Table 7. One thousand simulations of dynamic stress and strain were developed by using random variables having incorporated stress (σD), strain (εD), and material modulus (E_D).

Table 7. *μ, V and SD for dynamic stress, strain, and modulus of material (E).*

Variables	μ	V	SD
σ_D	$6.74*10^5$ psi (4647.06 MPa)	0.383	$2.58*10^5$ psi (1778.84MPa)
ε_D	0.024	0.38	0.0091
E_D	$2.65*10^5$ psi (1827.11 MPa)	0.237	$6.28*10^5$ psi (4329.91 MPa)

The results using 'RAND' function generated from random variables are shown in Figure 19, comprising integrity analyses conducted from the dynamic simulation results utilizing Table 4.

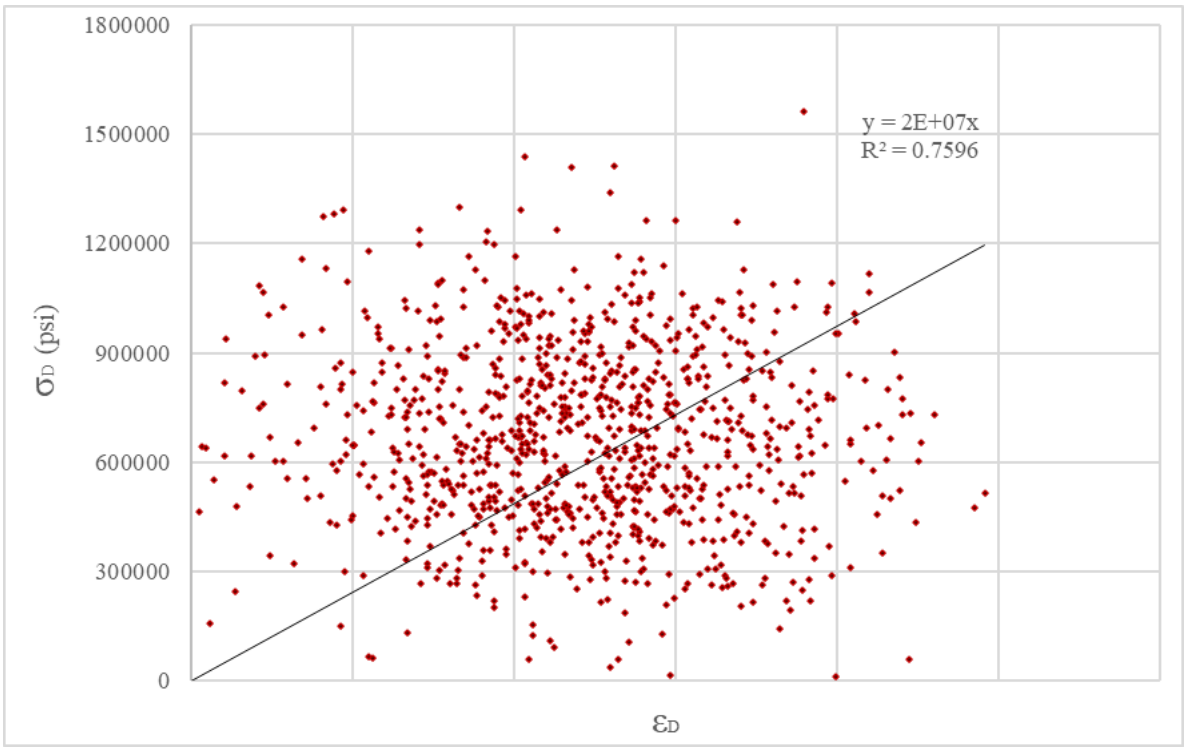

Figure 19. *Results of the Integrity Analysis from Dynamic Stress and Strain.*

From Figure 19, high-precision non-linear results from FE simulations are plotted via regression analysis to precisely capture the post impact dynamic performance of coupler using integrity analyses and is as given in Equation 14. This equation will help to provide high accuracy results via linear relationship with R^2 value of 0.76 from the regression result of specific impact scenario comprising post impact dynamic stress and strain concentration at coupler region.

$$g(\sigma_D, \varepsilon_D) = \sigma_D - 2 * 10^7 . \varepsilon_D \quad (14)$$

Where: σ_D is the dynamic stress concentration and ε_D is the corresponding dynamic strain at the coupler, and g is the post impact performance function as expressed in terms of stress and strain.

High precision dynamic simulations are carried out to capture the uncertainty of material performance and its behavior in terms of dynamic modulus of demand (beyond elastic limit) via regression analysis, and the results come up with a linear trend of performance function (g). The performance function (g) addresses linear trend to best capture of

dynamic stress and the corresponding dynamic strain concentration at coupler-rebar junction resulted by specific vehicle impact load comprising with a little flexible R^2 value due to large dataset.

5.3. Uncertainty Assessment Using Confidence Interval (CI)

Confidence Interval (CI) has been utilized to measure the degree of uncertainty for assessing non-linear results evaluated from dynamic simulation comprising stress (σ), strain (ε), and material modulus (E_D) of coupler materials resulted in during dynamic impact event. The uncertainty in the result of post impact dynamic event to capture the uncertainty involved is estimated using the confidence interval (CI) as exhibited in Table 6 is presented in Table 8. The CI results depict the uncertainties in material properties portraying a substantial variation with the assessment of post-performance behavior of the coupler material at specific impact load.

Table 8. *Results of CI.*

Variables	Confidence Value (CV)	Confidence Interval (CI)
σ_D (psi)	46199.18	$(7.15*10^5, 6.22*10^5)$
ε_D	0.000661	(0.0246, 0.0233)
E_D (psi)	46199.18	$(3.24*10^7, 3.23*10^7)$

5.4. Validation of Model

To validate the model for strain variations along with the stress concentrations at the steel rebar and coupler junctions, numerical (FE) simulation results from static analyses are compared with the experimental data comprising the strain and corresponding stresses from the published journal [6]. The model shows a good agreement and positive coherence with the experimental results in terms of the stress and strain relationship when apportioned load is transmitted and incurred from vehicle impact event on RC ABC bridge pier through grouted coupler. Validation of model proffers with the extracted experimental results and is as shown in Figure 20.

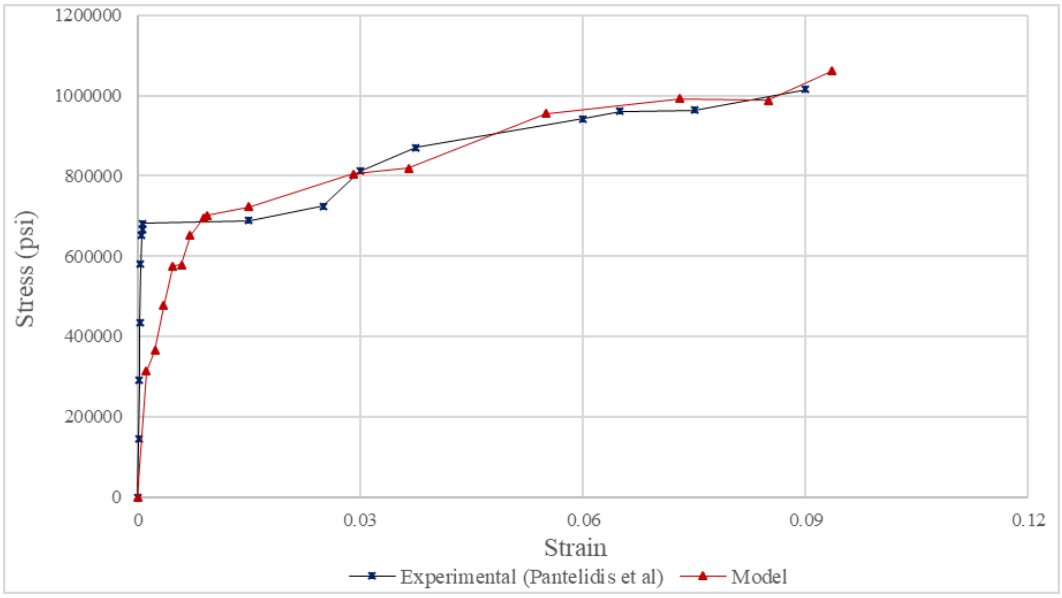

Figure 20. *Model validation with experimental data [6].*

Figure 20 can decently provide a compatible and acceptable normalized stress and strain results data of the coupler composite at specific high strain rate load and high deformation incurred by the coupler caused by semi-trailer impact via utilizing experimental and numerical results.

6. Discussions

In this research, an attempt has been carried out to predict the post impact performance of a RC bridge pier considering flexural response. In predicting its performance, splice-sleeve along with grouted coupler has been introduced in the bridge pier base. Stresses from vehicular impact are determined, and then compared the numerical results using FEA models for static and dynamic analyses. FEA models are generated in a conservative way where the apportioned axially compressive load and moment are incorporated and applied using area ratio ($A_{coupler}$ /A_{net}) to investigate the impact scenario of splice-sleeve under axial compression. Load has been generated and applied at the free end of the steel re-bar (Table 2). Stresses in the pier-base due (maximum stress concentration at the coupler end) to vehicular impact are analyzed for maximum stress concentration, strain compatibility and deformations. Stresses resulted due to impact and the dynamic amplification effect draw an insightful correlation between DIF's computed analytically (1.053) and numerically from the FE simulation (1.07) using the ratio of E-moduli (Dynamic modulus / Material modulus). FEM analyses present a little conservative result correlating proximity to the realistic. Due to variations in static and dynamic simulations results and complexities involved to capture material modulus as a post impact performance and exceedance of dynamic over static and material modulus, dynamic results for material modulus as demand are considered. The following observations perceived from this research are as shown:

1. The study depicts a little conservative result due to the boundary conditions deployed, and hence seems more realistic in design as far as dynamic effect is concerned. No further mesh refinement is necessary to predict split or spalling. Results shown from the exact solution while experiencing DIF of 1.053 (i.e., 5.3%), whereas material properties with a DIF of 1.07 (i.e., 7%) in terms of dynamic modulus of elasticity demands a little more conservative of 1.6% increment. FEM simulations are used to determine and validate DIF computed analytically. DIF computed by using analytical method and numerical simulations are quite similar, with 1.6% difference. This indicates high stress concentration in reinforcing steel bar-coupler junction. From steel deformation, it seems critical in steel bar due to conservative modeling.
2. Maximum stresses developed at the contact of steel rebar and coupler zone. This seems almost failure followed by large deformations in dynamic performance governing the control of material property. On the other hand, significant deformations are also observed along both the axes without failure in steel rebar for static performance.
3. The time dependent static strain and stress results are predicted from simulations and plotted by incorporating high strain rate. Dynamic performances of the steel and concrete composite system and its post impact behavior are further assessed and as shown in Figure 17 (a & b). Non-linear stress and strain concentration during specific vehicle impact is plotted (Figure 18) and the results are expressed in Equation 13. To precisely obtain stress and strain, linearized model is developed and captured via utilizing Equation 14. Integrity analysis of dynamic stress-strain resulted from simulation has been further undertaken through regression method. Results from regression analyses (Figure 19) are capable to capture material property while undergoing substantial deformation. From confidence interval (CI) the material property warrants about dynamic impact event as the dynamic demand (E_D) of coupler material exceeds the material modulus of elasticity (E).
4. Validation of model from the results of static stress and strain are compared with the experimental data and is as shown in Figure 20. This study also represents positive correlation of the model compared with the published data extracted from the experimental results. Risk analysis has been conducted using confidence interval and the results are shown in Table 8.

7. Conclusions

In reinforced concrete (RC) structures, piers are usually the most vulnerable members to collisions due to their exposed face and slender behavior. In particular, the desired characteristics and the associated impact performance levels of a structure during a vehicle collision are not well defined. Therefore, there is a need to assess the accountability of existing structures against such collisions, and proffer solutions to limit such susceptibility and enhance its performance level to withstand impact force. A specific method to assess the material capacity and demand of the coupler to its dynamic post impact performance are studied in this research. Based on the comparison of analytical studies, FEM simulation results, and its validation with the experimental results published in journals, the following conclusions can be drawn:

1. Studies are performed for comparing analytical and numerical analyses (FEM) comprising static and dynamic force models to assess moduli in demand to withstand high strain rate dynamic impact load and are compared with the corresponding material's moduli. To assess material performance, dynamic modulus is compared with the material modulus to compute DIF in demand, to come up with a good trade-off and agreement on material calibration utilizing approximate evaluation of the transmitted short duration dynamic impact loads.
2. Performance based studies of the impacted coupler are executed and presented for short duration impact where steel strain rates play significant role to determine the large deformation. Steel strain rate which is a function of DIF directly influences the resulting stresses in the

coupler-steel bar junction as shown in the Figures 18 and 19. This observation can help providing a fair agreement about material viability at impact, resolving shortcoming of material performance, and improving resilience and short duration impact behavior.

3. This research is also an attempt to investigate the material requirement for enhancing resistance. A reasonable 7 to 10% strength enhancement in material modulus is recommended for the cast-iron of splice-sleeve and steel bar to safely withstand high velocity vehicle impact without failure. This study instills an insightful idea and realistic correlation to accomplish material properties that can be safely predicted to ascertain essential criteria and perform useful calibration.
4. The integrity study utilizing simulation results will help to precisely detect high accuracy results at coupler from vehicle impact scenario. This will also provide improved information on material behavior and post impact performance for enhancing future calibration.
5. Risk analysis conducted using CI provides a clear understanding and precisely using the uncertainty parameters involved in analyzing connector at impact, determines the material's post impact behavior in withstanding specific dynamic impact performing as composite section. This concludes material's properties need to be upgraded.

However, high precision experimental studies involving various geometries, material properties and different impact scenarios are recommended before considering accelerated bridge constructed (ABC) piers for widespread use.

The data conversions undertaken in this research from US Customary to SI and vice-versa are shown in Table 9.

Table 9. *Conversion Chart for the US Customary to the Equivalent SI Units.*

US Customary	SI Unit
1 ksi	6.89 MPa (kN/mm^2)
1 ksi	6894.76 kN/m^2
1 kip-in	0.113 kN-m
1 kip	4.45 kN
1 lbs	0.00445 kN
1 mph	1.61 km/hr
1 ft-lb/sec	0.00136 kN-m/sec (1.36 N-m/sec)
1 in	0.0254 m (25.4 mm)
1 foot	0.3048 m (304.80 mm)
1 pci	271.4471 kN/m^3
1 psi	m^2

Abbreviations

f'_c	Concrete Strength
A_g	Gross c/s area of pier
A_{st}	Cross sectional area of reinforcing steel
A_{net}	Net cross-sectional area of pier
$A_{n,s}$	Cross-sectional area of each steel rebar
A_{CI}	Cross-sectional area of splice sleeve (cast iron)
A_{Grout}	Cross-sectional area of grout
$A_{coupler}$	Cross-sectional area of hollow splice-sleeve
E_{CI}	Material modulus of cast iron
E_{Grout}	Material modulus of grout, concrete
$E_{Concrete}$	Material modulus of concrete
E_{st}	Material modulus of reinforcing steel rebar
η	Energy dissipation
f_y	Yield strength of steel
P_n	Axial load of RC pier
$P_{n,s}$	Axial load of reinforcing steel rebar
$P_{n,s}$	Scaled-down design axial rebar load
σ_{dyn}	Dynamic flow stress
σ_y	Static flow stress
$\acute{\varepsilon}$	Quasi-static strain rate of steel re-bar
h	Pier diameter
h_I	Height of impact from pier base
σ	Stress
ε	Strain
E	Modulus of elasticity of coupler
σ_D	Stress
ε_D	Strain
E_D	Modulus demand of coupler at dynamic impact
ξ	Dynamic parameter
C and p	Material Constants
I_S	Static impact force
W	Vehicle weight
M_s	Static moment for each coupler
$M_{s,c}$	Static moment incurred by each coupler
$M_{dyn,c}$	Dynamic moment incurred by each coupler
M_{dyn}	Dynamic moment for each coupler
t	Impact duration (sec)
DIF	Dynamic Increase Factor
CI	Confidence interval
μ	Mean
SD	Standard deviation,
Z	Confidence level
N	Sample size

Acknowledgments

This publication was supported by NMB Splice Sleeve, North America, Inc. Any opinions, findings, and conclusions or recommendations expressed in this publication do not necessarily reflect the views of NMB Splice Sleeve.

Author's Contribution

Suman Roy[*1]: Conceptualized and developed the theoretical formalism, numerical models (FEM) and simulations, validation, performed the analytic calculations, writing draft and editing.

Funding Agencies

NMB Splice-Sleeve – North America, USA.

Availability of Data and Material

Some or all data, models, or code that support the findings of this study are available from the corresponding author upon reasonable request.

Conflicts of Interest

The author declares no conflicts of interest.

References

[1] (Rusty) Gray, G. T. (2012). "High-Strain-Rate Deformation: Mechanical Behavior and Deformation Substructures Induced." Annual Review of Materials Research, 42(1), 285–303.

[2] ACI. (2011). ACI 318-11: Building Code Requirements for Structural Concrete. American Concrete Institute.

[3] Actual Speeds on the Roads Compared to the Posted Limits. (2004). https://safety.fhwa.dot.gov/speedmgt/ref_mats/fhwasa09028/resources/actual%20speeds%20on%20roadtopostedlimits.pdf

[4] AFDC. (2018). "Vehicle Weight Classes & Categories." Alternative Fuels Data Centre, U.S. Department of Energy.

[5] Ameli, M. J., Brown, D. N., Parks, J. E., and Pantelides, C. P. (2016). "Seismic column-to-footing connections using grouted splice sleeves." ACI Structural Journal, American Concrete Institute, 113(5), 1021–1030.

[6] Ameli, M. J., and Pantelides, C. P. (2017). "Seismic analysis of precast concrete bridge columns connected with grouted splice sleeve connectors." Journal of Structural Engineering, American Society of Civil Engineers, 143(2), 4016176.

[7] ASTM. (2015). "A706/A706M − 15 Standard Specification for Low-Alloy Steel Deformed and Plain Bars for Concrete." Astm International, 1–6.

[8] Buth, C. E., Brackin, M. S., Williams, W. F., and Fry, G. T. (2011). "Collision Loads on Bridge Piers : Phase 2. Report of Guidelines for Designing Bridge Piers and Abutments for Vehicle Collisions." Austin, Texas, 100.

[9] Chopra, A. K. (2001). Dynamics of Structures, Theory and Applications to Earthquake Engineering. Upper Saddle River: Pearson-Prentice Hall.

[10] Cowper, G., and Symonds, P. (1957). "Strain hardening and strain-rate effects in the impact loading of cantilever beam." Brown University Division of Applied Mathematics, 1–46.

[11] Crosby, D., and Cheremisinoff, N. P. (1988). "Practical Statistics for Engineers and Scientists." Technometrics, 30(2), 234.

[12] Ebrahimpour, A., Earles, B. E., Maskey, S., Tangarife, M., and Sorensen, A. D. (2016a). Seismic performance of columns with grouted couplers in Idaho accelerated bridge construction applications. Idaho. Transportation Dept.

[13] Ebrahimpour, A., Earles, B. E., Maskey, S., Tangarife, M., and Sorensen, A. D. (2016b). "Seismic performance of columns with grouted couplers in Idaho accelerated bridge construction applications." (October).

[14] El-Tawil, S., Severino, E., and Fonseca, P. (2005). "Vehicle collision with bridge piers." Journal of Bridge Engineering, 10(3), 345–353.

[15] Feyerabend, M. (1988). "Hard transverse impacts on steel beams and reinforced concrete beams." University of Karlsruhe (TH), Germany.

[16] Fhwa. (2018). Concrete Bridge Shear Load Rating Synthesis Report. https://www.fhwa.dot.gov/bridge/loadrating/pubs/hif18061.pdf

[17] For, P., and By, A. (n.d.). GUIDELINES FOR PREPARING UDOT RESEARCH REPORTS.

[18] Furlong, R. W. (2014). "Design for Shear." 37.

[19] "Grouted Splice Sleeve Connectors for ABC Bridge Joints in High-Seismic Regions – Transportation Blog." (n.d.). https://blog.udot.utah.gov/2014/09/grouted-splice-sleeve-connectors-for-abc-bridge-joints-in-high-seismic-regions/ (Jul. 13, 2020).

[20] Hauksson, E., Kanamori, H., Stock, J., Cormier, M.-H., and Legg, M. (2014). "Active Pacific North America Plate boundary tectonics as evidenced by seismicity in the oceanic lithosphere offshore Baja California, Mexico." Geophysical Journal International Geophys. J. Int, 196, 1619–1630.

[21] ICC-ES Evaluation Report ESR-3433. (2014). https://icc-es.org/report-listing/esr-3433/

[22] ICC-ES Report. (2016). https://www.pwcva.gov/assets/2021-05/PA1201Att

[23] Jacob, G. C., Fellers, J. F., Starbuck, J. M., and Simunovic, S. (2004). Crashworthiness of Automotive Composite Material Systems.

[24] Kowalsky, M. J. (2000). "Deformation limit states for circular reinforced concrete bridge columns." Journal of Structural Engineering, American Society of Civil Engineers, 126(8), 869–878.

[25] Malvar, L. J. (1998). "Review of static and dynamic properties of steel reinforcing bars." ACI Materials Journal.

[26] Malvar, L. J., and Crawford, J. E. (1998). "Dynamic increase factors for steel reinforcing bars [C]." 28th DDESB Seminar. Orlando, USA.

[27] Pantelides, C. P., Ameli, M. J., Parks, J. E., and Brown, D. N. (2014). Seismic evaluation of grouted splice sleeve connections for precast RC bridge piers in ABC. Utah Department of Transportation.

[28] Roy, S., Unobe, I., and Sorensen, A. D. (2021). "Vehicle-Impact Damage of Reinforced Concrete Bridge Piers: S State-of-the Art Review." J. Perform. Constr. Facil., American Society of Civil Engineers 2021, 35(5): 03121001, 35(5).

[29] Roy, S., and Sorensen, A. (2021a). "Energy Based Model of Vehicle Impacted Reinforced Bridge Piers Accounting for Concrete Contribution to Resilience." 18th International Probabilistic Workshop: IPW 2020, Springer Nature, 301.

[30] Roy, S., and Sorensen, A. (2021b). "A Reliability Based Crack Propagation Model for Reinforced Concrete Bridge Piers Subject to Vehicle Impact." 18th International Probabilistic Workshop: IPW 2020, Springer Nature, 95.

[31] Roy, S., Unobe, I. D., and Sorensen, A. (2022a). "Damage characterization and resilience optimization of reinforced concrete bridge piers under vehicle impact." Advances in Bridge Engineering, 3(1), 16.

[32] Roy, S., Unobe, I. D., and Sorensen, A. D. (2022b). "Investigation of the performance of grouted couplers in vehicle impacted reinforced concrete ABC bridge piers." Advances in Bridge Engineering, SpringerOpen, 3(1), 1–30.

[33] Sanders, David H. (2012). " Evaluation of the Seismic Performance of Circular and Interlocking RC Bridge Columns under Bidirectional Shake Table Loading." 15th World Conference on Earthquake Engineering (15WCEE), (September 2018).

[34] Sharma, H., Gardoni, P., and Hurlebaus, S. (2015). "Performance-Based probabilistic capacity models and fragility estimates for RC columns subject to vehicle collision." Computer-Aided Civil and Infrastructure Engineering, 30(7), 555–569.

[35] Sharma, H., Hurlebaus, S., and Gardoni, P. (2012). "Performance-based response evaluation of reinforced concrete columns subject to vehicle impact." International Journal of Impact Engineering, 43, 52–62.

[36] "Speed limits in the United States - Wikipedia." (n.d.). https://en.wikipedia.org/wiki/Speed_limits_in_the_United_States (Apr. 24, 2020).

[37] Tavio, T., and Tata, a. (2009). "Predicting Nonlinear Behavior and Stress-Strain Relationship of Rectangular Confined Reinforced Concrete Columns with ANSYS." Civil Engineering, 11(1), 23–31.

[38] Tazarv, M., and Saiidi, M. S. (2016). "Seismic design of bridge columns incorporating mechanical bar splices in plastic hinge regions." Engineering Structures, Elsevier, 124, 507–520.

[39] Thomas, R. J., Steel, K., and Sorensen, A. D. (2018). "Reliability analysis of circular reinforced concrete columns subject to sequential vehicular impact and blast loading." Engineering Structures, Elsevier, 168, 838–851.

[40] Zhao, X., Wu, Y.-F., Leung, A. Y., and Lam, H. F. (2011). "Plastic hinge length in reinforced concrete flexural members." Procedia Engineering, Elsevier, 14, 1266–1274.

[41] Zhou, D., Li, R., Wang, J., and Guo, C. (2017). "Study on Impact Behavior and Impact Force of Bridge Pier Subjected to Vehicle Collision." Shock and Vibration, 2017, 1–12.